J Mater Sci (2006) 41:4883–4891
DOI 10.1007/s10853-006-0050-7

Effect of NbC and TiC precipitation on shape memory in an iron-based alloy

N. Stanford · D. P. Dunne

Received: 28 July 2005 / Accepted: 26 September 2005 / Published online: 27 May 2006

Abstract This paper examines the effects of TiC and NbC precipitation and prior cold rolling on the shape memory behaviour of an iron-based alloy. A precipitate-free alloy was used as a reference to investigate the relative contributions of prior-deformation and precipitation on shape memory. Heat treatment of the Nb- and Ti-containing alloys at 700 °C and 800 °C resulted in carbide precipitates between 120 nm and 220 nm in diameter. Bend testing of these samples showed a marginal increase in shape memory compared to the precipitate-free alloy. Under these conditions TiC precipitation exhibited slightly better shape memory than for NbC. However, this small increase was over-shadowed by the marked increase in shape memory that can be produced by subjecting the alloys to cold rolling followed by recovery annealing. When processed in this way, fine carbides are formed in the Ti- and Nb-containing alloys during the heat treatment. For particles >25 nm in diameter the shape memory is unaffected, but, it was found that small <5 nm particles have a detrimental effect on shape memory due to pinning of the martensite plates, thereby inhibiting their reversion to austenite. The optimum shape memory was observed in the precipitate-free alloy after cold rolling and recovery annealing.

Introduction

Fe–Mn–Si-based alloys are a well-known shape memory alloy system. The austenitic fcc (γ) parent phase can transform to a hexagonal martensite phase (ε) by the formation of stacking faults. The ε martensite reverts to austenite on heating, thus imparting shape memory properties [1–3].

These alloys are known to require ''training'' to achieve the optimum shape memory effect (SME). This training involves several cycles of deformation and annealing, usually in tension, before the alloy is tested for its SME [3, 4]. Much recent research activity has been directed at the development of alloys and processing methods that do not require this training procedure. Alloys that can be precipitation strengthened have received much recent attention because Kajiwara et al. have shown that precipitation of NbC particles in austenite can significantly increase the SME without the need for training [5–9]. The first report of this behaviour [5] showed that precipitation of NbC from the austenite resulted in an increase in the strain recovery from 1 to 2%. This result was then improved [6, 8, 9] by refining the particle size by pre-rolling the microstructure before precipitation heat treatment. This has yielded strain recovery of around 4%, which is said to be better than a five times training cycle [8]. This pre-rolling is essentially a training step, in compression instead of the more commonly used tensile test. What is not explicitly detailed in Refs. [8] and [9] is the effect of the rolling and annealing treatment on an alloy that does not produce particles during heat treatment. In light of the two separate effects, training and precipitation, it is the aim of this paper to elucidate the relative contributions of each to the SME.

The iron alloy system is known to form a range of carbides under the appropriate thermal conditions and composition ranges. Since NbC is claimed to have a positive effect on SME, it seems likely that other precipitates may also have a positive effect. Therefore, another

N. Stanford (✉) · D. P. Dunne
Faculty of Engineering, University of Wollongong, Wollongong, NSW 2522, Australia
e-mail: standford@uow.edu.au

aim of the paper is to establish if other carbides are capable of increasing the SME like NbC, and to quantitatively compare them. In this work Ti was chosen because, like Nb, it is a strong carbide former known to readily form TiC.

Method

The base stainless alloy used in this study was made in a 2.6 kg ingot by induction melting under an argon atmosphere. Small pieces of approximately 40 g in mass were sectioned from the as-cast slab. To these small pieces, alloying additions of Ni, Nb and Ti were made by arc-melting. Both Nb and Ti are strong ferrite formers, and an additional 2% Ni was added to stabilize the austenite phase in the Ti- and Nb-bearing alloys. The slight variations in the Mn and Cr concentrations shown for the alloy compositions in Table 1 are likely to be the result of segregation during the solidification of the original base alloy. The carbon content was measured on the base alloy using spectrographic analysis, and is assumed to be the same in the other alloys. The other elements listed in Table 1 were measured using energy dispersive spectroscopy (EDS) on a scanning electron microscope (SEM).

The as-cast alloys were hot rolled at 900 °C to a thickness of 0.9 mm. Samples of rolled strip were solution treated at 1100 °C for 1 h under flowing argon atmosphere, then water quenched. After solution treatment, samples were divided into two groups; the first group was heat treated at various times and temperatures to promote precipitation of carbide, and the second group was cold rolled and then subjected to the same heat treatments. A range of heat treatment times and temperatures were used, and these are shown in Table 2. All cold rolling was carried out to 7% reduction in thickness at room temperature.

For optical and electron microscopy the samples were polished by standard metallographic techniques, and the martensite induced by polishing was removed by a final polish with colloidal silica. Optical and SEM samples were etched using acid ferric chloride (5% ferric chloride, 25% HCl, 70% H_2O).

The shape memory effect (SME) was measured using bend tests involving pre-strains between 1% and 6% and a sample thickness of ~900 μm. The range of pre-strains was accomplished by bending samples around different bend radii. The pre-strain was taken as the maximum tensile/compressive strain, and is determined by the equation:

$$\varepsilon = \frac{1}{(2R/h) + 1} \quad (1)$$

where ε is conventional strain, R is bend radius, and h is sample thickness.

The shape was recovered by annealing in a muffle furnace at 400 °C for 15 min. After the samples had been recovery annealed the residual strain (ε_r) remaining due to incomplete recovery was calculated using Eq. (1). The percentage recovery was determined by the equation:

$$\%\text{Recovery} = (\varepsilon - \varepsilon_r)/\varepsilon \quad (2)$$

Electron microscopy was carried out on a Leica 440 SEM and a JEOL JEM 2011 transmission electron microscope (TEM). TEM samples were prepared with a Struers Tenupol jet-polisher using a solution of 5% perchloric acid in acetic acid at room temperature and a voltage of 30 V. The transformation behaviour of the samples was investigated using a TA Q100 differential scanning calorimeter (DSC) at a scan rate of 10 °C/ min.

Results

Microstructure

The microstructures of all three alloys were essentially the same, and a typical example is shown in Fig. 1. The austenite grain size was approximately 100 μm, and there was a high density of recrystallization twins throughout the microstructure. This micrograph was taken from a bend test sample, and the large amount of martensite evident is the result of this bending deformation. In the Ti-containing samples there were some TiN particles present that had probably formed during arc-melting. These particles did not appear to change size or morphology during the heat treatments.

Table 1 Alloy compositions in weight percentage measured using EDS

Name	C*	Mn	Si	Ni	Cr	Fe	Ti	Nb
Base alloy	0.06	11.4	4.5	4.7	9.8	Bal	–	–
Nb alloy	0.06	12.9	4.5	6.7	9.5	Bal	–	0.5
Ti alloy	0.06	12.5	4.5	6.2	9.4	Bal	0.5	–

*Measured using spectrographic analysis

Table 2 List of heat treatments carried out on the base alloy, and the Ti- and Nb-containing alloys

	Base alloy	Nb alloy	Ti alloy	Heat treatment
	x	x	x	Austenitized 1100 °C, water quenched
Group 1	x	x		300 °C, 15 min, water quenched
		x	x	500 °C, 3 h, water quenched
		x	x	700 °C, 15 min, water quenched
	x	x	x	800 °C, 15 min, water quenched
			x	800 °C, 1 h, water quenched
Group 2	x	x		Cold rolled 7%, 300 °C, 15 min, water quenched
	x	x	x	Cold rolled 7%, 500 °C, 3 h, water quenched
	x	x	x	Cold rolled 7%, 700 °C, 15 min, water quenched
	x	x	x	Cold rolled 7%, 800 °C, 15 min, water quenched
			x	Cold rolled 7%, 800 °C, 1 h, water quenched

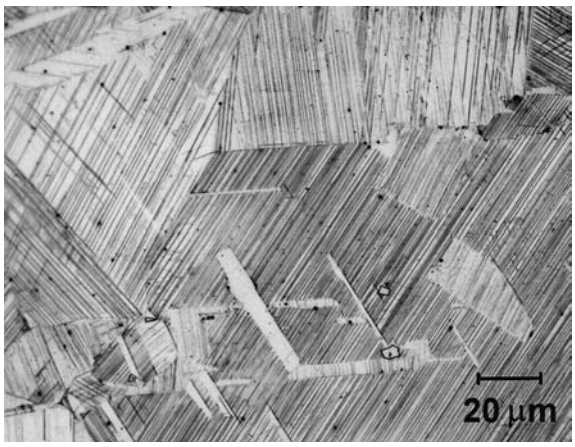

Fig. 1 Optical micrograph of Ti-containing sample after heat treatment at 800 °C for 15 min, followed by deformation by bending to a strain of 4%

Transmission electron microscopy (TEM) was used to examine the size and distribution of carbide precipitates after each of the heat treatments, and these are summarised in Table 3. There were no carbide precipitates found under any heat treatment condition in the base alloy. In this base alloy, the most likely carbide formers are Cr and Fe, and presumably these require longer treatment times than used here. No carbide precipitates were found in any alloy after heat treatment for 3 h at 500 °C.

It is evident from Table 3 that cold rolling prior to heat treatment significantly decreases the particle size. This is consistent with previous work on similar alloys [7]. When pre-rolled, the stacking faults induced by deformation act as nucleation sites for carbides during the heat treatment, and this refines the carbide size. When no prior rolling is given there are fewer nucleation sites and the carbides coarsen and tend to be more clustered.

In the absence of prior cold rolling, the TiC particles were very similar in size and distribution after treatment at 700 °C and 800 °C. In both cases the particles were approximately 200 nm in diameter. For the Nb-containing alloy, heat treatment at 800 °C produced larger particles than treatment at 700 °C, the sizes being 180 nm and 120 nm, respectively.

After cold rolling (7% reduction) followed by heat treatment at 800 °C, the NbC and TiC precipitates had a similar size and distribution, with the average particle diameter being 30 nm. However, after cold rolling and heat treatment at 700 °C the NbC particles were much smaller, less than 5 nm in diameter, and were only visible by the Moiré fringe patterns (Fig. 2a). After the same treatment the TiC particles were much larger compared to the NbC particles, being about 25 nm in diameter (Fig. 2b). Figure 2a also shows that the NbC particles can be associated with martensite plates. It was commonly observed that clusters of these fine precipitates were associated with martensite plates, and that regions without precipitates were often free of martensite. The martensite is probably an artefact produced during the sample preparation, and retained by particle pinning.

Table 3 Approximate sizes of carbide particles measured using TEM

Prior deformation	Heat treatment	Base alloy	NbC (nm)	TiC (nm)
No rolling	3 h, 500 °C	No pptn	No pptn	No pptn
	15 min, 700 °C	No pptn	120	200
	15 min, 800 °C	No pptn	180	220
7% cold rolled	3 h, 500 °C	No pptn	No pptn	No pptn
	15 min, 700 °C	No pptn	<5	25
	15 min, 800 °C	No pptn	30	30

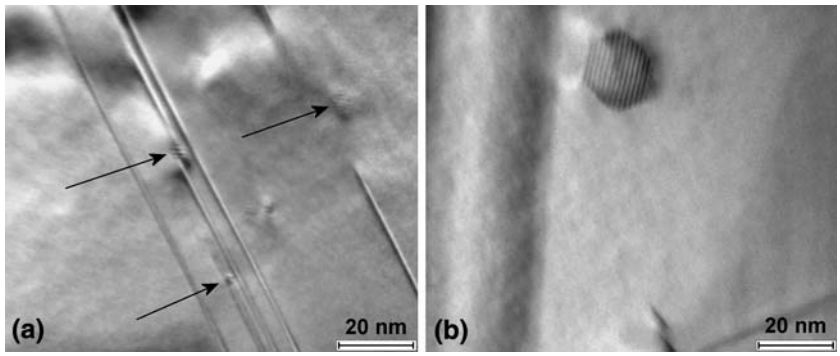

Fig. 2 TEM micrographs of (**a**) Nb-containing and (**b**) Ti-containing alloys after 7% cold rolling followed by heat treatment at 700 °C for 15 min. Micrographs shown at same magnification. Scale bar = 20 nm

Transformation behaviour

The transformation temperatures of selected samples, measured using DSC, are shown in Fig. 3. The A_s temperatures are around 30 °C lower in the Nb-containing alloy, and around 40 °C lower in the Ti-containing alloy, compared to the base alloy. The M_s was measured to be −23 °C in the base alloy, but was not able to be measured in the other two alloys. The M_s is likely to have been suppressed below the temperature limit of the DSC in the Nb- and Ti-containing alloys, which is −50 °C in the instrument used here. Assuming the same A_s–M_s interval as the base alloy, the Nb- and Ti-containing alloys would be predicted to have M_s temperatures of −57 °C and −67 °C, respectively. Annealing at 800 °C did not have a marked effect on the A_s in any of the three alloys. Cold rolling to 7% reduction followed by annealing at 800 °C was not found to have a significant effect on the transformation temperatures, other than to raise the A_s by around 5–10 °C. Minor changes in the transformation temperatures would not be expected to have a significant effect on the SME.

Shape memory of austenitized samples

The shape memory of the base alloy, Nb alloy and Ti alloy after austenitizing heat treatment at 1100 °C is shown in Fig. 4. This treatment is effectively a solution treatment, and it is evident that the alloys show very similar shape memory behaviour. For clear representation, a line has been fitted to the austenitized samples in Fig. 4, and this line is reproduced, where relevant, in following shape memory graphs for easy comparison of results. This reference line is referred to as the austenitized shape memory response (ASMR) curve.

Effect of annealing on SME of base alloy

Figure 5 shows the SME of the base alloy after annealing for 15 min at 300 °C and at 800 °C. There is little differ-

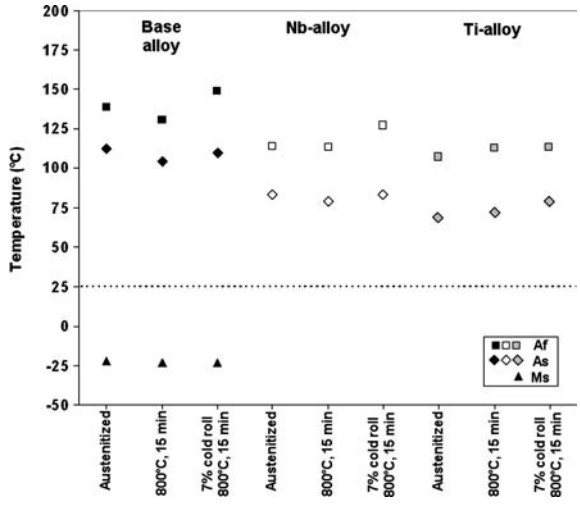

Fig. 3 Transformation temperatures measured using DSC for the base, Nb-, and Ti-containing alloys

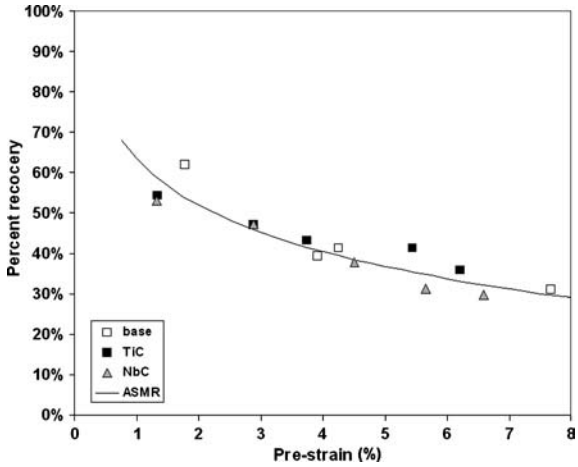

Fig. 4 Shape memory (% recovery) of the base alloy, Ti-containing alloy and Nb-containing alloy after austenitizing heat treatment at 1100 °C. Line of best fit shows austenitized shape memory response curve (ASMR) for comparison in the following sections

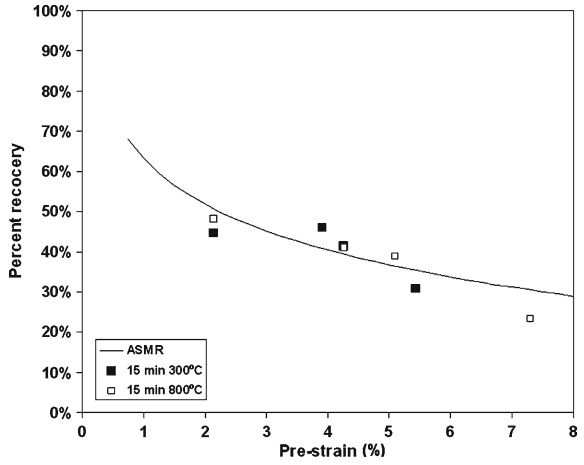

Fig. 5 Shape memory (% recovery) of the base alloy after annealing for 15 min at 300 °C and 800 °C. Solid line shows ASMR curve

ence between the SME of the annealed samples and the ASMR curve. This is consistent with the DSC results that showed little change in the transformation temperatures with annealing.

Effect of cold rolling and annealing on SME

The precipitate-free base alloy was cold rolled to 7% reduction and heat treated for the same times and temperatures that were adopted for the precipitation treatments. The effect of treatment temperature on the SME is shown in Fig. 6. As can be seen the best results were obtained after recovery treatment at 700 °C and 800 °C. Compared to the higher temperatures the SME is markedly lower after treating at 300 °C and 500 °C and is similar to the ASMR curve.

For the base alloy, cold rolling to 7% reduction and recovery of the martensite at 300 °C resulted in a hardness increase of approximately 60 HV compared to the austenitized sample (Fig. 6b). The hardness of the base alloy was slightly higher than that of the austenitized condition after 15 min at 800 °C.

Effect of precipitation on SME

The SME for Ti and Nb alloy samples that were heat treated only, with no prior cold rolling, is shown in Fig. 7. For the Nb alloy the best results were obtained after treatment at 800 °C for 15 min. Treatment at 700 °C and 500 °C resulted in shape recovery similar to that of the reference austenitized state (ASMR curve). However, heat treatment at 300 °C resulted in poorer SME than for the austenitized condition.

For the Ti alloy (Fig. 7b), the SME was generally higher than for the Nb alloy and was best after heat treatment at 800 °C. Treatment for 15 min at 800 °C showed basically the same SME as after treatment for 1 h at 800 °C. The SME decreased with decreasing heat treatment temperature. Although these heat treatments did in fact produce carbide precipitates as they were designed to (e.g., Fig. 2), the hardness measurements (Fig. 8) did not show a marked increase with precipitation.

Effect of pre-rolling and precipitation on SME

The SME for samples that were cold rolled and then precipitation heat-treated are shown in Fig. 9. For the Nb-containing alloy, the best results were achieved after

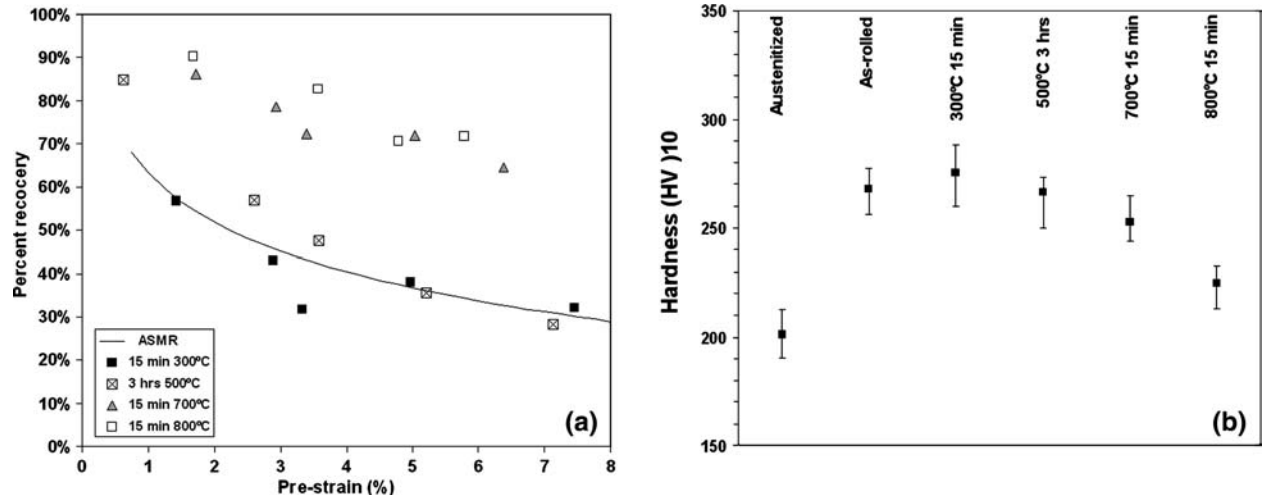

Fig. 6 (**a**) Shape memory (% recovery) of the base alloy after cold rolling 7% and heat treatment at the times and temperatures indicated. Solid line shows ASMR curve. (**b**) Vickers hardness (10 kg) of samples from (**a**)

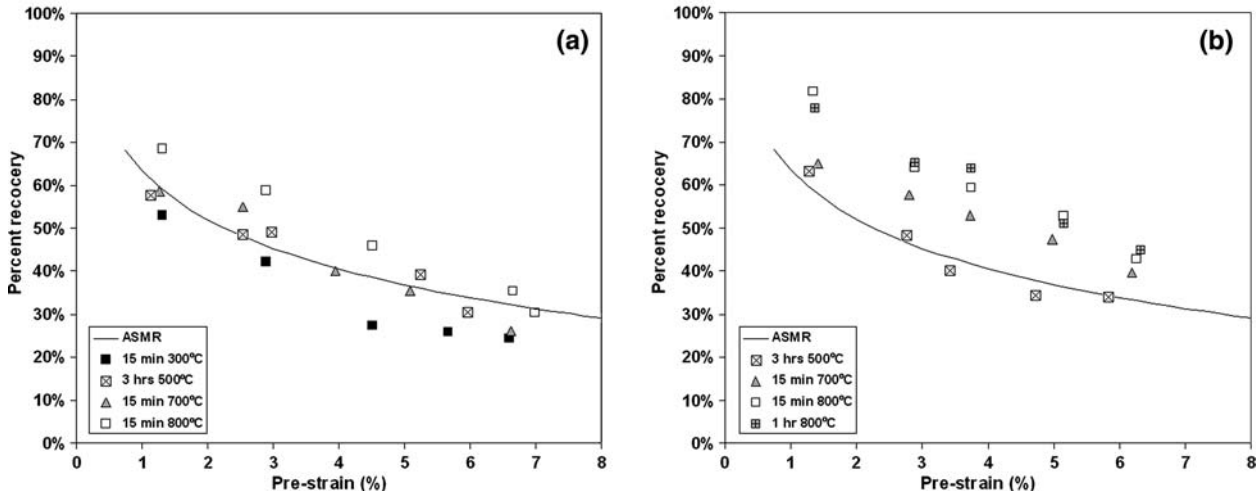

Fig. 7 Shape memory after heat treatment for (**a**) Nb-containing alloy and (**b**) Ti-containing alloy. Solid lines show ASMR curve

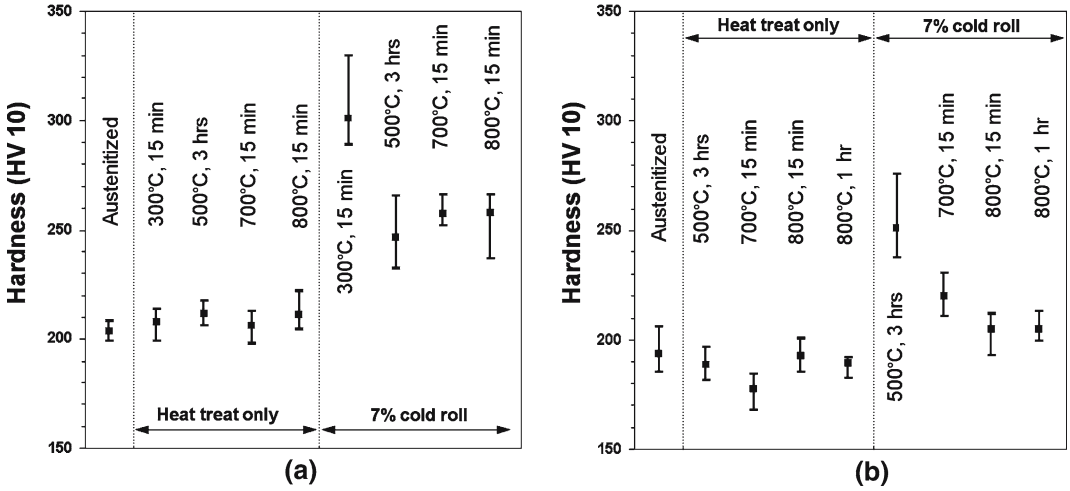

Fig. 8 Vickers hardness of (**a**) Nb-containing alloy and (**b**) Ti-containing alloy after the specified heat treatments

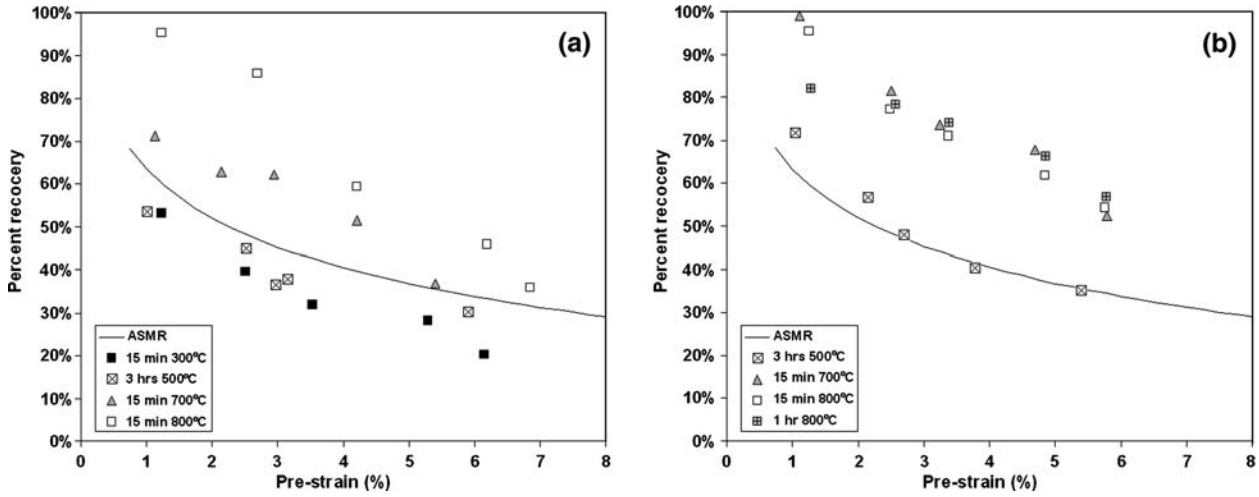

Fig. 9 Shape memory of (**a**) Nb-containing and (**b**) Ti-containing alloy after cold rolling to 7% reduction and heat treatment. Solid lines show ASMR curve

cold rolling and heat treatment at 800 °C for 15 min. Treatment at 700 °C after rolling significantly reduced the SME compared to 800 °C. After treatment at 300 °C and 500 °C the samples showed a slightly lower SME response than the austenitized samples (ASMR curve).

For the Ti-containing alloy, high SME was achieved for 15 min at 700 °C, 15 min at 800 °C and 1 h at 800 °C. Reducing the heat treatment temperature to 500 °C significantly reduced the SME.

Discussion

Effect of NbC and TiC precipitation

Figure 10 compares the shape memory of the Nb and Ti alloys that were not cold rolled prior to heat treatment. This figure indicates that precipitation marginally improves SME compared with the austenitized condition (ASMR curve) and that TiC slightly out-performs the NbC as a shape memory enhancing precipitate.

In both the Nb and Ti alloys the heat treatments at 800 °C did not increase the hardness significantly, even though TEM showed that precipitation did in fact occur. This suggests that the increased SME is not primarily a result of austenite strengthening. Both the work of Kajiwara et al. [5] and others [7] show that the most effective heat treatment temperature for NbC precipitates is 800 °C. In Ref. [7] it is shown that the SME is enhanced by increasing the size of the precipitates by over-aging for 10 h at 800 °C. After such a long time at temperature it is not likely that that the particles are coherent with the matrix, and since experimental evidence shows that larger precipitates are beneficial, it seems that coherency is not a major contributor to good SME in these types of alloys.

During pre-strain to stress induce martensite, precipitates act as stress concentrators within the austenite matrix, and it has already been suggested [5, 10] that NbC particles may act as nucleation sites for martensite. It is likely that the same martensite variant is activated at each particle throughout the austenite grain, increasing the likelihood of one variant being present in each grain. This is a possible cause of the small increase in shape recovery found in samples heat treated at 700 °C and 800 °C to produce coarse carbide precipitates (Fig. 10).

Effect of pre-rolling and recovery on SME

Figure 6 shows that shape memory can be dramatically increased by cold rolling and recovery. This is not a new phenomenon in iron-based shape memory alloys. It is well established that ‘‘training’’ is an effective method of increasing the shape memory. This training usually involves up to five successive treatments of tensile deformation to around 5% strain followed by a recovery anneal. The shape memory is then tested in the same tensile geometry, and typically increases the recovered strain from around 2% to 4%. In this study, the cold rolling and annealing is analogous to the tensile training normally carried out on these alloys.

It is also shown in Fig. 6 that a high recovery temperature is required before rolling can be a successful training step. Deformation followed by annealing at 300 °C or 500 °C does not produce an increase in SME, while annealing at 700 °C or 800 °C does increase the SME. In tension, it has been shown [11] in a similar alloy that

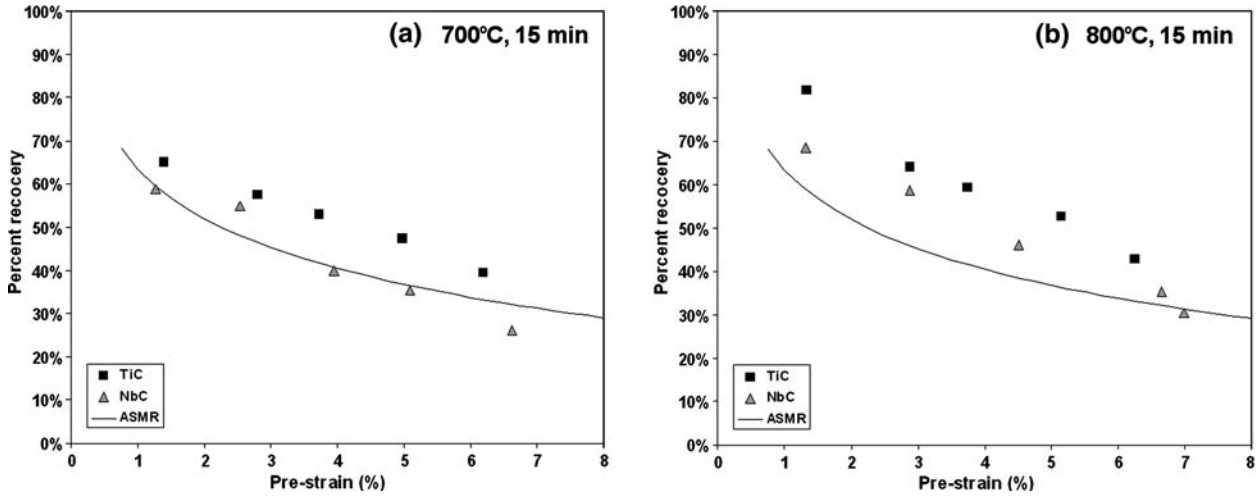

Fig. 10 SME of the Ti-containing and Nb-containing alloys after heat treatment at (**a**) 700 °C for 15 min and (**b**) 800 °C for 15 min. Solid lines show ASMR curve

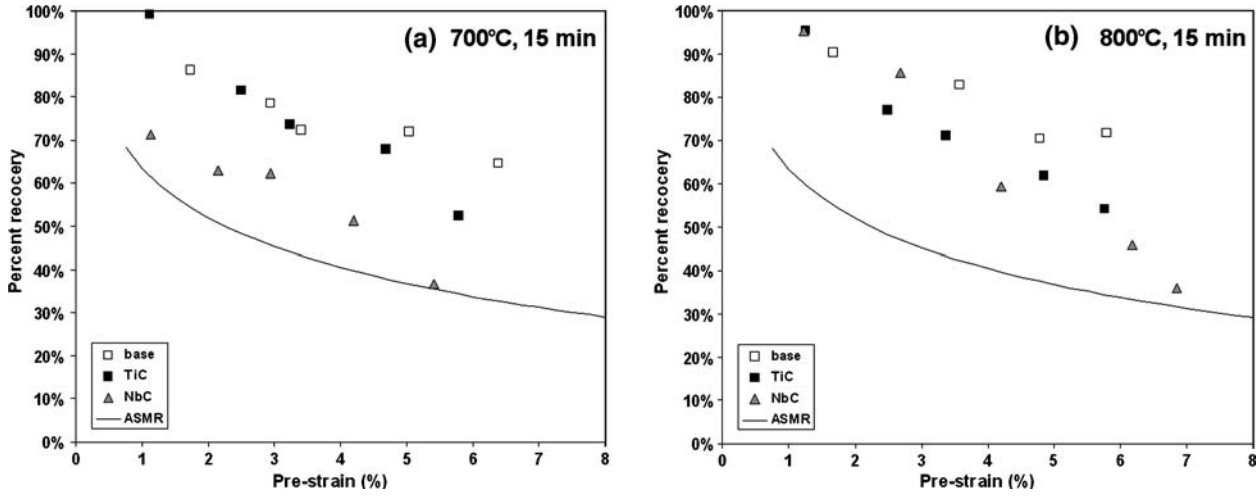

Fig. 11 Shape memory of all three alloys after cold rolling and heat treatment at (**a**) 700 °C for 15 min and (**b**) 800 °C for 15 min. Solid lines show ASMR curve

500 °C or above is effective for recovery treatment, and that temperatures of 400 °C or below are not high enough for recovery. In this study the precipitate-free base alloy, after 7% cold rolling, required a recovery temperature of 700 °C or above to increase shape memory. Recovery temperatures ≤500 °C are too low to produce good shape memory when rolling is used as the deformation mode.

Figure 11 shows the shape memory behaviour for all three alloys after cold rolling and heat treatment. It is evident that after heat treatment at 800 °C the shape memory for all samples is similar at pre-strains less than 4%. However, at higher strains the sample with no precipitates performs slightly better than those containing precipitates. TEM showed that the size of the precipitates was much the same after heat treatment at 800 °C in both the Ti- and Nb-containing alloys. This is consistent with the shape memory being similar in both alloys. However, after treatment at 700 °C the TiC alloy clearly performs better than the NbC alloy (Fig. 11a). The major difference between the precipitates in this instance is that the TiC particles are much larger than in the Nb alloy. This result is consistent with the preceding discussion that it is advantageous for SME to have larger particles. TEM also showed that clusters of martensite plates and dislocation arrays were often associated with NbC particles, and that adjacent to these regions there were large areas of austenite without martensite plates or precipitation (e.g., Fig. 2). It appears that the fine coherent NbC precipitates are able to pin martensite plates, and retard their reversion. This manifests itself as a reduction in the shape memory behaviour (Fig. 11a). This conclusion, that very fine precipitates are detrimental to SME, is at odds with previously published studies on NbC precipitation. However, in this study we have shown that pre-rolling followed by heat treatment is a far more effective method of enhancing SME than precipitation alone (Figs. 6, 9). It is therefore likely that the enhanced SME described in Refs. [6], [8] and [9] does not result solely from precipitation of very fine (4–6 nm) NbC precipitates, but is more likely to be a result of the pre-rolling step given before precipitation heat treatment.

Conclusions

This paper has examined the effect of two variables: carbide precipitation, and pre-rolling, on the shape memory behaviour of an iron-based shape memory alloy.

For the Nb- and Ti-containing alloys, with no prior cold rolling, the following conclusions are drawn.

- Nb and Ti in solution do not enhance SME.
- Precipitation of both NbC and TiC marginally increases the shape memory behaviour of Fe–Mn–Si-base shape memory alloys relative to the solution treated alloy.
- TiC appears to be slightly more effective as a shape memory enhancing precipitate than NbC.
- Carbides between 120 nm and 220 nm in diameter have a positive effect on shape memory. It is proposed that these particles act as stress concentrators in the austenite matrix and promote the nucleation of martensite during pre-strain. These particles are large enough that they do not exert a pinning effect during the martensite to austenite reversion.

For 7% cold rolling followed by heat treatment at 700 °C or 800 °C, the main conclusions are as follows.

- Cold rolling before precipitation heat treatment is advantageous to shape memory by virtue of the rolling being a ‘‘training’’ step.

- Although precipitation increases SME compared to the solution treated case, when cold deformation and annealing is applied the training effect dominates the SME. This training step is just as effective in precipitate-free alloys as it is in precipitate-containing alloys at low (<4%) pre-strains.
- The presence of precipitates has a detrimental effect on SME at high pre-strains relative to the precipitate-free alloy.
- Compared to the precipitate-free alloy, precipitation of fine carbides, less than 5 nm in diameter, has a detrimental effect on shape memory. It is proposed that these fine particles pin martensite plates and inhibit their reversion during recovery annealing.

Acknowledgements The work carried out in this paper was funded by the Australian Research Council *Discovery Grant* programme. The authors would also like to thank Mr. Greg Tillman for his assistance with metallography, and Dr. David Wexler for his support with transmission electron microscopy.

References

1. Sato A, Chishima E, Soma K, Mori T (1982) Acta Metall 30:1177
2. Sato A, Chishima E, Yamaji Y, Mori T (1984) Acta Metall 32:539
3. Kajiwara S (1999) Mat Sci Eng A A 273–275:67
4. Otsuka H, Murakami M and Matsuda S (1989) In: Doyama M, Sōmiya S, Chang R (eds) Proceedings of the MRS international meeting on advanced materials, vol 9, Tokyo, Japan 1998, Materials Research Society, Pittsburgh, p 451
5. Kajiwara S, Liu D, Kikuchi T, Shinya N (2001) Scripta Mater 44:2809
6. Baruj A, Kikuchi T, Kajiwara S, Shinya N (2003) J Phys IV 112:373
7. Dong Z, Liu W, Chen J, Wang D (2003) J Phys IV 112:389
8. Baruj A, Kikuchi T, Kajiwara S, Shinya N (2004) Mat Sci Eng A A 378:333
9. Baruj A, Kikuchi T, Kajiwara S, Shinya N (2002) Mat Trans 43:585
10. Baruj A, Kikuchi T, Kajiwara S (2004) Mat Sci Eng A A 378:337
11. Li H (1996) PhD Thesis, University of Wollongong